

# Quasi-Optical Power Combining Using Mutually Synchronized Oscillator Arrays

Robert A. York, *Student Member, IEEE*, and Richard C. Compton, *Member, IEEE*

**Abstract**—A quasi-optical method for solid-state power combining is discussed, with application to high-power millimeter-wave generation. The approach uses two-dimensional planar arrays of weakly coupled oscillators. Limiting the strength of the coupling avoids multifrequency moding problems and simplifies the design. A radiating element is embedded in each oscillator so that the power combining is accomplished in free space. The concept has been demonstrated with two prototype arrays, one using Gunn diodes and the other MESFET's. A theoretical description of the coupled-oscillator arrays is also presented for design purposes, and is used to investigate phasing problems and stability. Experiments indicate that in-phase operation is facilitated by using a quasi-optical reflector element, which influences the operating frequency and coupling between the elements. Equivalent isotropic radiated powers of 22 W at 1% efficiency for a 16-element Gunn array and 10 W at 26% efficiency for a 16-element MESFET array have been obtained at X band.

## I. INTRODUCTION

CURRENT research interest in millimeter-wave systems is motivated by several frequently cited advantages, such as smaller antennas, wider bandwidths, and better resolution for imaging and radar systems. However the natural progression from the microwave to millimeter-wave spectrum has been hindered in many cases by the lack of compact, reliable, high-power solid-state sources at these wavelengths. High-power vacuum-tube devices are available, but their large size and weight and their high voltage requirements often preclude their use. Unfortunately, fundamental device physics demands that millimeter-wave semiconductor devices be extremely small, and their power handling capacity is correspondingly reduced. In order to compete with vacuum tubes, solid-state sources must therefore use large numbers of devices. For example, state-of-the-art traveling-wave tubes can produce better than 100 W at 100 GHz [1]; comparable results for a solid-state system would require at least 200 IMPATT's or 1000 Gunn diodes [2].

Several different approaches to power combining have been developed by researchers during the last two decades [3]. In practice the task is complicated by multimoding

problems. Traditional combining techniques using hybrid 3 dB couplers or large numbers of devices in a resonant cavity [4] have fundamental limits regarding efficiency and the number of devices that can be combined. The limitations arise from unavoidable circuit losses and/or the requirement of a small cavity to avoid multimode problems. Circuits which have been carefully designed to minimize these effects have proved superior to tubes for some applications [5], but these architectures become impractical as the frequencies approach 100 GHz.

More recently a planar quasi-optical approach has been suggested for combining the output powers of millimeter devices [6]. The transverse dimensions of quasi-optical systems can be quite large, which accommodates many devices without the problem of multifrequency operation. Where traditional combining techniques require nonreciprocal elements to prevent device interaction, the quasi-optical arrays depend on the controlled interaction of the devices for proper operation. The power combining takes place in free space; hence high combining efficiencies (close to 100%) are possible. These arrays are expected to have application in a wide range of frequencies, up to the terahertz range using suitable devices [7].

Two types of quasi-optical arrays have been reported to date [27]. One uses a distributed oscillator approach in which the devices are mounted in a periodic grid structure [8], [9], [30] and placed in an open quasi-optical cavity. This approach is analogous to a laser, in which the distributed oscillator system acts as the active gain medium. A second approach, which is the focus of this paper, involves arrays of weakly coupled individual oscillator elements [26]. This system forms a classical antenna array in which each radiating element is itself a free-running oscillator. The array elements are synchronized through mutual coupling mechanisms (free space and/or surface waves). The strength of the coupling between elements is limited to ensure that each element operates close to its free-running state; hence the operating frequency is solely determined by the design of the individual oscillator elements. This technique is modular, as more elements can be added to increase the power without altering the operating frequency. The approach is free of the multimoding problem which plagues other methods, since each element is designed to operate at only one frequency. In this paper we discuss the design and operation of coupled-oscillator arrays, and present experimen-

Manuscript received October 30, 1990; revised January 22, 1991. This work was supported by the U.S. Army Research Office and by General Electric.

The authors are with the School of Electrical Engineering, Cornell University, Ithaca, NY 14853.

IEEE Log Number 9144293.

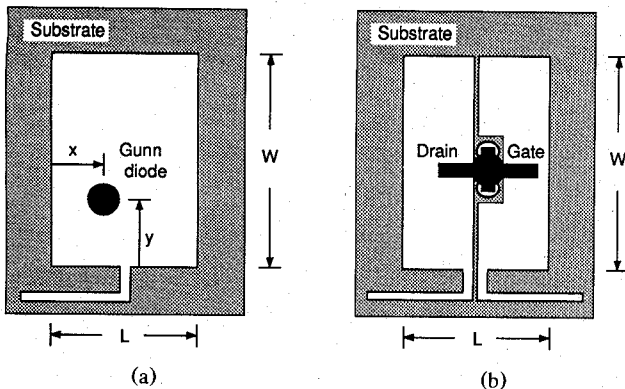


Fig. 1. Active patch antennas using two- and three-terminal devices. (a) A Gunn or IMPATT diode is mounted between the ground plane and the patch. (b) An FET is mounted across the narrow gap, with source leads grounded through the substrate. Bias lines are also shown. These elements are simple to design and easy to fabricate, making them attractive for use in large arrays.

tal results from two 16-element X-band systems using Gunn diodes and MESFET's.

## II. ACTIVE RADIATING ELEMENTS

The important components in these power-combining arrays are the individual oscillator elements, consisting of an active device (Gunn, IMPATT, RTD, FET, etc.) integrated directly into a radiating element. Several novel architectures have appeared in the literature [10]–[14] which creatively incorporate an active device in a planar microstrip antenna. Important figures of merit are the output power, efficiency, and packing density. The experimental arrays described later were constructed using two different active microstrip patch antenna designs, one with a Gunn diode [10] and the other with a MESFET [14], as shown in Fig. 1. The patch antenna is a useful structure for this purpose, since the devices can be integrated vertically and heat-sinking is facilitated by the ground plane.

The Gunn/patch element was constructed using the topology of Fig. 1(a). The device is located at the point where its impedance is matched to that of the patch. This position can be found using a first-principles time-domain simulation of the device [15] and a suitable model for the patch input impedance (such as the cavity model). Alternatively, a semiempirical approach can be used [16], where an approximate impedance is assumed for the device and the proper location is found using this impedance. The semiempirical method is convenient for hybrid X-band circuits, but more involved computer modeling is important for millimeter devices which must be integrated monolithically into the antenna and hence are more difficult and expensive to make. Bias is applied at a low impedance point on the patch.

A FET/patch element was also developed for power-combining arrays [14], and is shown in Fig. 1(b). This structure is not a conventional patch antenna, since it uses two low-impedance microstrip lines coupled by a narrow gap. The device is mounted in a common-source

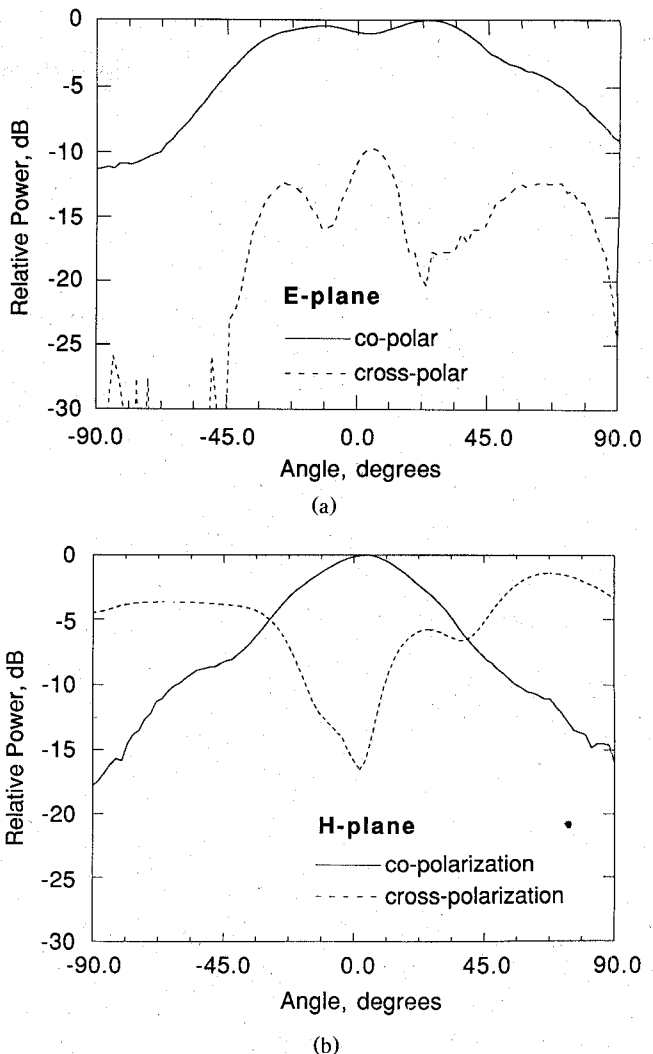


Fig. 2. Typical (a) *E*-plane and (b) *H*-plane patterns for a 7.6 GHz Gunn/patch element. The dashed curves are cross-polarization measurements. High cross-polarization is due to the large size of the packaged device compared with the antenna.

configuration across this gap, with the source leads grounded through the substrate. The feedback capacitance from the gap is sufficient to make the device unstable (and hence useful as an oscillator), while the open-circuited lines provide a good conjugate match to the load (radiation resistance). The FET/patch element has a demonstrated efficiency of 26%, but otherwise behaves like the Gunn/patch element. For this reason, only data for the single Gunn/patch element will be presented here.

Typical radiation patterns for a Gunn/patch element are shown in Fig. 2. This element measured 0.45 by 0.65 in., with the diode 0.15 in. from the edge, and was fabricated on 60 mil,  $\epsilon_r = 4.1$  substrate. Commercially available low-power MA/COM packaged Gunn diodes (MA 49104) were used in this work. Typical bias was 12 V at 250 mA, with an overall dc-to-RF efficiency of 1%. Linear polarization and measured antenna patterns were consistent with expected patch behavior. The high cross-polarization in the *H*-plane measurement indicates excess-

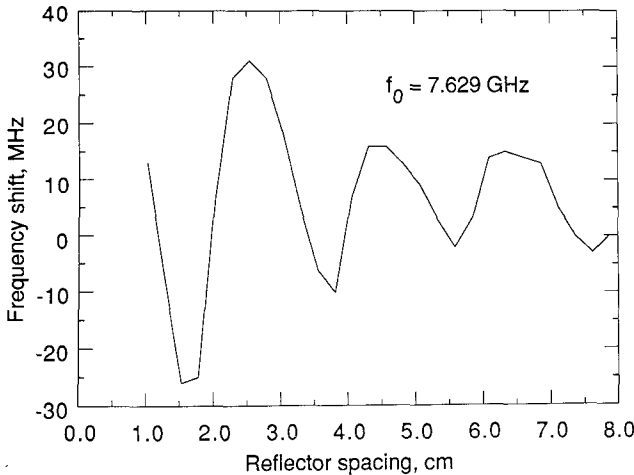


Fig. 3. Frequency tuning versus reflector placement for the Gunn/patch circuit. This curve was measured at 13 V bias, with a 1 in. dielectric slab ( $\epsilon_r = 4$ ). The periodicity corresponds to approximately half a free-space wavelength.

sive coupling to other patch modes, which is attributed to the large size of the diode package in relation to the antenna; this effect should be reduced in a monolithically fabricated array [10], since no bulky package would be used.

The tuning curves (frequency and output power versus bias voltage) for the circuit were very similar to other published measurements. Bias tuning can be used to compensate for small discrepancies between the elements, which is important because the proper operation of the array requires that the elements have nearly identical characteristics. For an array of elements, a partial reflector (such as a dielectric slab) positioned above the array facilitates the mutual injection locking of the devices and helps establish the proper phase relationships between the elements. Fig. 3 shows the measurements of a single Gunn/patch element when a dielectric slab is moved above the device. This behavior can be explained using the basic injection locking theory described below.

### III. COUPLED OSCILLATOR THEORY

An analysis of systems using coupled or “inter-injection-locked” microwave oscillators has been published [17], [18]. These analyses are elegant but are impractical for power-combining arrays containing hundreds or thousands of elements. In what follows, a simple treatment of the problem is presented based on Adler’s equation for injection locking [19], in order to gain some physical insight into the design and operation of these arrays. This approach was motivated by recent work in low-frequency coupled oscillators [22], [23]. In that work, an unusual mathematical model was postulated for the oscillator, which dissociates amplitude and phase dynamics. It was then argued that the steady-state behavior is a function of the phase dynamics alone, and after introducing a suitable coupling term, a compact analytical result for coupled oscillators was derived. However, the models were

chosen without any correspondence to physical reality, and the coupling mechanism was assumed instantaneous, which is not a valid assumption at high frequencies. In this section it will be shown that a similar set of equations can be derived with Adler’s equation as the starting point, including the effects of coupling delay between elements. Note that we adopt virtually the same notation as [23] in the following equations.

In order to neglect amplitude dynamics, weak coupling between the elements is assumed (the meaning of “weak” will be made clear later). This implies that the individual oscillators are only slightly perturbed from their free-running state by the presence of the other oscillators. This assumption leads naturally to Adler’s equation for injection locking [19]–[21], which is given by

$$\frac{d\phi_0}{dt} = -\frac{A_{\text{inj}}}{A_0} \frac{\omega_0}{2Q} \sin(\phi_0 - \psi_{\text{inj}}) + (\omega_0 - \omega_{\text{inj}}) \quad (1)$$

where  $\phi_0$  = phase of oscillator,  $\psi_{\text{inj}}$  = phase of injected signal,  $\omega_0$  = free-running frequency of oscillator,  $\omega_{\text{inj}}$  = frequency of injected signal from an external or neighboring oscillator,  $A_0$  = free-running amplitude of oscillator (voltage),  $A_{\text{inj}}$  = amplitude of injected signal (voltage), and  $Q$  = the external  $Q$  of the oscillator circuit. The phase of the oscillator is defined relative to the injected signal frequency, so that the steady-state solution,  $d\phi_0/dt = 0$ , corresponds to the oscillator being frequency-locked to the injected signal. Adding the injected frequency to both sides of (1) and noting that  $\omega = \omega_{\text{inj}} + d\phi_0/dt$  = the instantaneous frequency of the oscillator yields

$$\omega = \omega_0 \left[ 1 - \frac{A_{\text{inj}}}{A_0} \frac{1}{2Q} \sin(\phi_0 - \psi_{\text{inj}}) \right]. \quad (2)$$

For mutually synchronized arrays, (2) must be modified to include the effects of coupling delay and several simultaneous injected signals. First, the coupling between individual oscillators can be expressed in terms of a complex coupling coefficient. This is similar to the scattering parameter  $s_{ij}$  of the circuit connecting the two oscillators  $i$  and  $j$  (reciprocity is assumed,  $s_{ij} = s_{ji}$ ). The magnitude and phase of this coupling coefficient are written separately as  $\lambda_{ij} \exp(j\Phi_{ij})$ . Secondly, superposition is used to account for several simultaneously injected signals. Incorporating the above for a system of  $N$  oscillators gives a modified form of Adler’s equation for the  $i$ th oscillator,

$$\omega = \omega_i \left[ 1 - \sum_{j \neq i}^N \frac{\lambda_{ij}}{2Q_i} \frac{A_j}{A_i} \sin(\phi_i - \phi_j + \Phi_{ij}) \right], \quad i = 1, 2, \dots, N \quad (3)$$

where the instantaneous frequency  $\omega$  of oscillator  $i$  is the same for all oscillators in the system *at synchronization*. Equation (3) describes a set of equations which can be used to determine the steady state of the system. If the free-running parameters are given, the unknowns are the phase differences and operating frequency of the array.

Conversely, one can solve for the frequencies and amplitudes which give a prescribed phase distribution.

Some simple analytical results can be derived from (3) by considering a linear chain of oscillators with only nearest-neighbor interactions (the more general situation of a two-dimensional array is similar but notationally more complicated). Assuming that the coupling is the same between adjacent elements in the array,  $\lambda_{ij} \equiv \lambda$  and  $\Phi_{ij} \equiv \Phi$ . Furthermore, let  $Q \equiv Q_i$ ,  $\lambda' \equiv \lambda/2Q$ ,  $\rho_i \equiv A_{i-1}/A_i$ , and  $\Delta\phi_i \equiv \phi_i - \phi_{i-1}$ . The set of governing equations becomes

$$\omega = \omega_i [1 - \lambda' \rho_i \sin(\Phi + \Delta\phi_i) - \lambda' \sin(\Phi - \Delta\phi_{i+1})/\rho_{i+1}]$$

$$n = 1, 2, \dots, N. \quad (4)$$

Note that  $\rho_1 = 1/\rho_{N+1} = 0$ . This is the same form obtained in [23], except for the presence of the coupling phase term. However this additional term renders the equations unsolvable by conventional linear techniques. To solve these equations, further assumptions must be made such as a small angle restriction where  $\sin(\Delta\phi_i) \approx \Delta\phi_i$ , or a nonlinear root-finding procedure could be used. For small numbers of elements, the equations can be solved analytically.

In general there are many possible phase distributions which satisfy this set of equations, but not all are stable solutions. Stability of these modes can be investigated using a perturbation analysis. Recalling that  $\omega = \omega_{\text{inj}} + d\phi_i/dt$ , a new differential equation is obtained.

$$\frac{d}{dt} \Delta\phi_i = \omega_i [1 - \lambda' \rho_i \sin(\Phi + \Delta\phi_i) - \lambda' \sin(\Phi - \Delta\phi_{i+1})/\rho_{i+1}]$$

$$- \omega_{i-1} [1 - \lambda' \rho_{i-1} \sin(\Phi + \Delta\phi_{i-1}) - \lambda' \sin(\Phi - \Delta\phi_i)/\rho_i]. \quad (5)$$

The phase is then perturbed by a small amount by letting  $\Delta\phi_i \rightarrow \Delta\phi_i + \delta_i$ . After some algebra this leads to

$$\frac{d}{dt} \delta_i = a_i \delta_{i-1} + b_i \delta_i + c_i \delta_{i+1} \quad i = 2, 3, \dots, N$$

where

$$a_i = \lambda' \rho_{i-1} \omega_{i-1} \cos(\Phi + \Delta\phi_{i-1})$$

$$b_i = -\lambda' \omega_i \rho_i \cos(\Phi + \Delta\phi_i) - \lambda' \omega_{i-1} \cos(\Phi - \Delta\phi_i)/\rho_i$$

$$c_i = \lambda' \omega_i \cos(\Phi - \Delta\phi_{i+1})/\rho_{i+1}. \quad (6)$$

This is of the form of a matrix equation,  $d\delta/dt = A\delta$ , where  $A$  is a tridiagonal matrix and  $\delta$  is a column vector with elements  $\delta_i$ . A stable solution for the phase distribution requires  $\delta$  to decay with time. This is satisfied when all the eigenvalues of  $A$  have negative real parts. In all of the numerical solutions of (4) and (6) which have been carried out so far, the stability criterion (6) has eliminated all but one or two of the possible modes given by (4). This observation has resisted an analytical justification so far.

It has also been observed that for certain values of the coupling phase there are no stable modes of operation.

#### IV. POWER COMBINING WITH COUPLED OSCILLATOR ARRAYS

To illustrate the theory and derive some important qualitative results, consider a simple chain of four similar oscillators. From (4),

$$\omega = \omega_1 [1 - \lambda' \sin(\Phi - \Delta\phi_2)]$$

$$\omega = \omega_2 [1 - \lambda' \sin(\Phi + \Delta\phi_2) - \lambda' \sin(\Phi - \Delta\phi_3)]$$

$$\omega = \omega_3 [1 - \lambda' \sin(\Phi + \Delta\phi_3) - \lambda' \sin(\Phi - \Delta\phi_4)]$$

$$\omega = \omega_4 [1 - \lambda' \sin(\Phi + \Delta\phi_4)] \quad (7)$$

assuming that the oscillator amplitudes are approximately the same so that  $\rho_i \approx 1$ . This is usually a good approximation in practice. From (7), if the amplitudes are similar, then the final oscillation frequency of the array will lie within the locking range of each oscillator; that is, the locking ranges of every oscillator must overlap to some extent. Since these are weakly coupled oscillators, the locking bandwidth is small; hence the elements must be nearly identical to satisfy (7). It is important to note, from (2), that since the oscillator phase undergoes a  $180^\circ$  variation over the locking range, small differences in the free-running frequencies can have a large effect on the solution. Assuming perfectly identical oscillators ( $\omega_1 = \omega_2 = \omega_3 = \omega_4$ ) gives

$$\sin(\Phi - \Delta\phi_2) = \sin(\Phi + \Delta\phi_2) + \sin(\Phi - \Delta\phi_3)$$

$$\sin(\Phi + \Delta\phi_2) + \sin(\Phi - \Delta\phi_3) = \sin(\Phi + \Delta\phi_3) + \sin(\Phi - \Delta\phi_4)$$

$$\sin(\Phi + \Delta\phi_3) + \sin(\Phi - \Delta\phi_4) = \sin(\Phi + \Delta\phi_4). \quad (8)$$

This shows that end effects will be important, at least for small arrays, since the elements on the periphery see quite different injection signals. There are many possible solutions to (8); for phase-coherent power combining, of most interest is the solution for which  $\Delta\phi_2 = \Delta\phi_3 = \Delta\phi_4 = 0$ . For this solution, (8) is satisfied when  $\Phi = n\pi$ , where  $n = 0, 1, 2, \dots$ . From the stability analysis, the following eigenvalue equation is obtained:

$$\begin{vmatrix} -2\cos\Phi - \epsilon & \cos\Phi & 0 \\ \cos\Phi & -2\cos\Phi - \epsilon & \cos\Phi \\ 0 & \cos\Phi & -2\cos\Phi - \epsilon \end{vmatrix} = 0. \quad (9)$$

The eigenvalues  $\epsilon$  can have negative real parts only if  $\cos\Phi > 0$ , so a stable, in-phase mode is only possible if  $\Phi = 0, 2\pi, \dots$ . If free-space coupling is predominant, this means that the elements must be spaced at multiples of one wavelength. Such spacing is generally unacceptable because of grating lobes in the antenna patterns. Furthermore, it has been shown that close spacing is desirable for large arrays for efficient power combining [6]. We have found that placing a quasi-optical reflector element (such

as a dielectric slab) over an array can influence the coupling between the elements and thereby facilitate phase-coherent operation. An alternative view is that the reflector forms a resonant cavity with the array, and the elements interact via a cavity mode. The effect of this reflector on a single element has been shown in Fig. 3, but more work must be done to incorporate this element into the previous theory. Consistent with the weak-coupling assumption, the reflectivity of this element must be small. Note that the use of a reflector is not a novel idea [6], [9], but the above analysis demonstrates that it is not necessary to the operation of these arrays, although in practice it greatly simplifies the design. Instead of a reflector element, a microstrip coupling circuit could be designed to provide a weak coupling signal at the required phase angle. This has been demonstrated experimentally [13] using one-wavelength microstrip lines on GaAs to connect IMPATT oscillators.

It is desirable to quantify the assumption of weak coupling for design purposes. This can be done to a rough approximation by considering (3). Replacing the sine term by 1 gives the maximum possible deviation of the oscillator from its free-running state. Taking this as a measure of the coupling strength, and assuming a frequency deviation of 10% of the locking bandwidth as the demarcation of weak coupling, gives

$$M\lambda \leq 0.1 \quad (10)$$

where identical oscillators have been assumed and  $M$  is the number of elements coupling into each oscillator. For a chain of oscillators with nearest-neighbor coupling,  $M = 2$  and the constraint (10) is given by  $\lambda \leq 0.05$ , or  $-13$  dB.

The assumption of identical oscillators is generally difficult to realize in practice. Most oscillators can be designed to have some tunability with bias voltage, and this can be used to ensure identical oscillation frequencies (this does not guarantee stability, however). Individual bias to each element also allows the system to degrade gracefully—for multiple devices on a single bias, failure of one device often leads to failure of all of the devices. However, individual bias to all the elements of a large array containing several hundred devices is impractical. Another possibility is shown in Fig. 4, where several devices are connected (via low-pass sections or chokes) to the same bias line. This can be done if the oscillators are designed to oscillate at the same frequency for a given bias. For packaged devices this is difficult to achieve, but monolithically fabricated arrays could yield the required uniformity between elements to make this technique possible. Parasitic patch elements on the array periphery might be used to ensure identical operating characteristics, although this has not yet been tested.

Fig. 5 shows the experimental results using the different array configurations of Fig. 4. Both four-element linear arrays use the FET/patch element described previously. The element spacing is  $0.58\lambda_0$  in Fig. 5(a) and

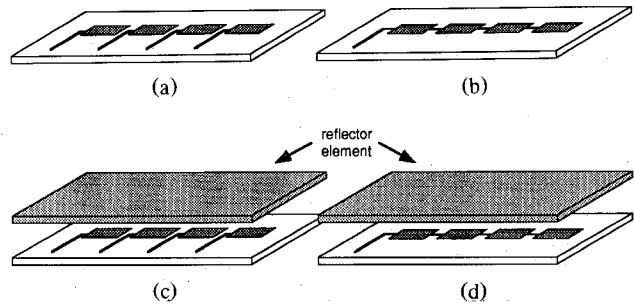


Fig. 4. Some different array configurations which have been considered. (a) The individual bias allows for device nonuniformities and graceful degradation, but the bias lines quickly use up substrate space. (b) Driving multiple devices from a single bias line is less flexible, but may be possible for monolithic arrays. (c), (d) Addition of a reflector element can greatly simplify the design and operation of these arrays.

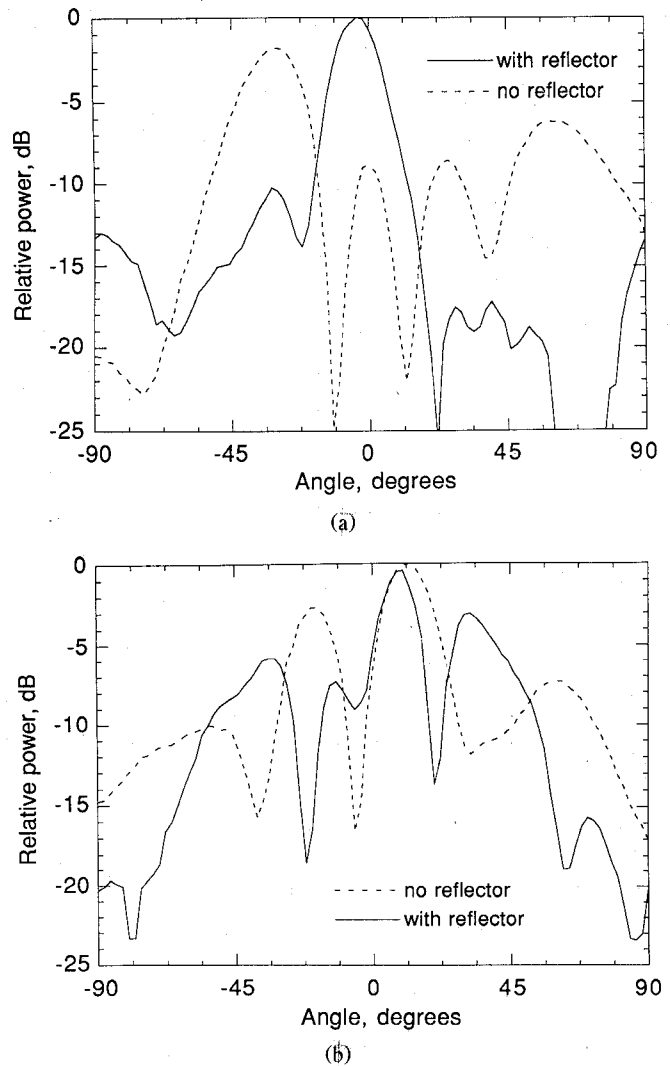


Fig. 5. *H*-plane patterns for two four-element arrays. (a) Each element is individually biased. Without the reflector the stable mode gives a main lobe at  $-30^\circ$ ; addition of a reflector enforces the in-phase mode. (b) The elements are connected to the same bias line as in Fig. 4, with low-pass sections between the elements. Owing to small differences in the operating points of each oscillator, it is difficult to establish a mode with the elements all in phase.

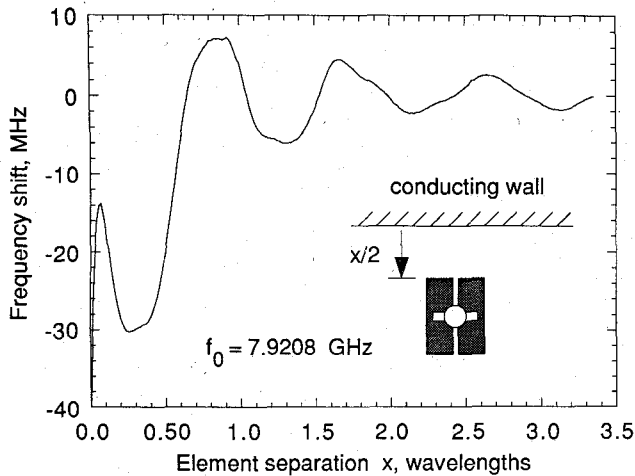


Fig. 6. Frequency shift for the coupled oscillator measurement scheme, using FET/patch elements with dimensions 11 mm by 15 mm on 93 mil,  $\epsilon_r = 2.33$  substrate. Coupling parameters can be extracted from this curve. At small element separations, the coupling becomes too strong and the theory is not valid.

0.72 $\lambda_0$  in Fig. 5(b). In Fig. 5(a), the elements were each tuned to a frequency of 7.921 GHz. The element spacing is such that the stable mode without a reflector gives a main lobe at  $-30^\circ$  from broadside. A 2.5-cm-thick dielectric slab ( $\epsilon_r = 4$ ) was positioned above the array to give the indicated pattern, which corresponds to the elements operating in phase. Note that much different patterns would be obtained for other reflector positions, owing to the resultant change in oscillator coupling; the patterns shown here represent the closest to in-phase operation. The second case of all elements on the same bias line is shown in Fig. 5(b).

Recently a convenient technique for measuring the mutual coupling between adjacent oscillator elements has been described [25], which can be used to determine the coupling coefficients in (4) experimentally. In this technique, two identical oscillators which are  $180^\circ$  out of phase are simulated by imaging a single oscillator using a metal sheet perpendicular to the plane of the patch. The operating frequency of the system is monitored while the distance between the metal mirror and the oscillator is varied. From (4), the frequency variation is described by  $\Delta f/f_0 = \lambda'(x)\sin\Phi(x)$ , where  $f_0$  is the free-running frequency of the oscillator, and  $\lambda'$  and  $\Phi$  are functions of the element spacing,  $x$ . A coupling measurement using the FET/patch element is shown in Fig. 6. Note that at very small separations the coupling may become too strong and the theory would not be valid.

The functional dependencies of the coupling parameters described by the curve in Fig. 6 were found to be well approximated by equations of the form  $\lambda'(x) = A/x$  and  $\Phi(x) = -2\pi x/\lambda_0$ , where  $A$  and  $b$  are constants and  $x$  is the element spacing. (Note that the element spacing here is the distance between adjacent edges of neighboring elements, whereas the element spacing quoted in the array designs is the distance between element centers.) This expression for  $\Phi$  occurs if free-space coupling is

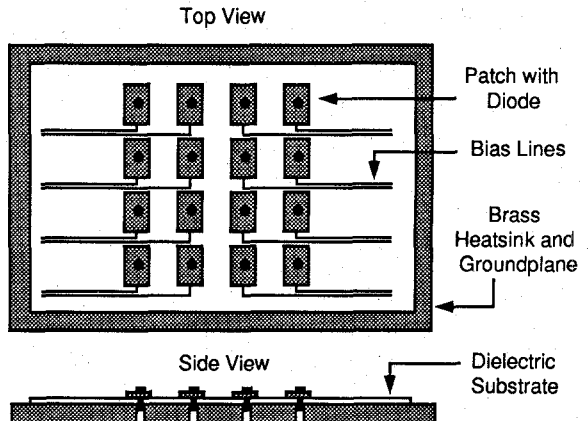


Fig. 7. Diagram of Gunn diodes mounted into a  $4 \times 4$  array of microstrip patches. The brass block serves as a groundplane, heatsink, and dc bias return. Individual bias to each element is applied at an RF null.

predominant [24], which is expected since the simulation does not faithfully include coupling through the substrate.

Although the coupling is important to the operation of small arrays, this may not be as critical for extremely large arrays, where end effects are smaller. In this case the steady-state phase distribution will be mostly determined by stability considerations, which give a range of values for the allowed coupling phase.

## V. EXPERIMENTAL ARRAY RESULTS

### A. $4 \times 4$ Gunn Diode Array

The first experimental array of weakly coupled oscillators was a 16-element array using Gunn diodes, shown in Fig. 7 [26]. The individual elements were designed semiempirically, as described previously. This array design uses individual bias to each device, which was required owing to device nonuniformities. Elements of the array are spaced half a free-space wavelength apart, a distance which was initially selected based on curves in [6]. The array was designed on a 60 mil substrate with  $\epsilon_r = 4.1$ .

Each diode was first biased, one at a time, to establish a common operating frequency. These individual biases were then applied simultaneously. Single-frequency operation was verified with a spectrum analyzer, as shown in Fig. 8(b). Spectra resembling Fig. 8(a) result when the elements are not all in synchronization. (This effect has been fully explained using Adler's equation [20, 21].) Slight differences in diode characteristics and diode placements made the simultaneous injection locking a delicate operation. As previously suggested, the addition of a 1-in.-thick dielectric slab ( $\epsilon_r = 4.0$ ) above the array facilitated the injection locking.

The individual elements exhibited a frequency tuning from 9.5 to 10.0 GHz versus bias voltage. The best results for the array were obtained at a frequency of 9.6 GHz, which is within 4% of the design frequency. Sharp patterns in both the  $E$  and the  $H$  plane corresponding to a directivity of 17 dB were measured at this frequency (Fig.

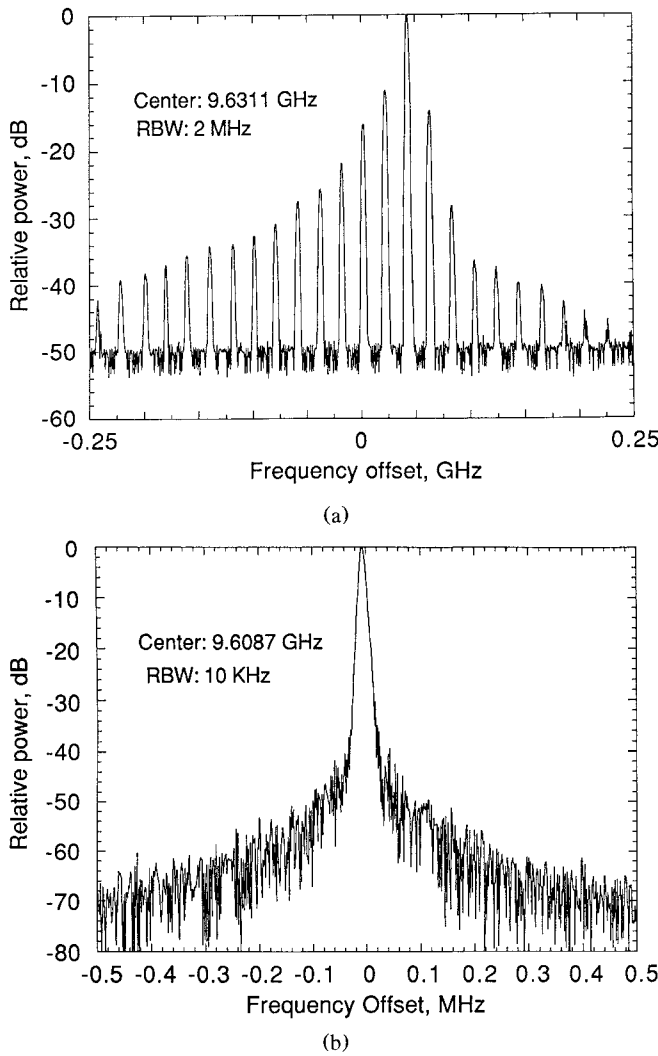


Fig. 8. (a) Spectrum of the Gunn array on the threshold of synchronization and (b) at full synchronization. These measurements were made with the dielectric reflector in place.

9), and indicate in-phase operation. Some frequency tuning was observed by adjusting the position of the dielectric slab, but this effect is limited to the maximum locking range of the array ( $\approx 100$  MHz) and also changes the radiation patterns substantially.

A maximum received power of 9.6 mW was obtained at a distance of 1.1 m from the array, using a 19 dB pyramidal horn. The total radiated power, estimated from the measured  $E$  and  $H$  patterns, was 415 mW. (Note that the number quoted for total radiated power here is slightly larger than that given in [26], owing to a numerical error in a previous calculation.) The method of estimating total power from the principal radiation patterns is admittedly inaccurate, but based on comparisons with theoretical models we believe that the figure presented here may actually underestimate the total power by as much as 16%. This total power figure gives 26 mW per device, which is consistent with the 25 mW rating of the diodes—considerably more power could be obtained using devices of higher power. The above data correspond

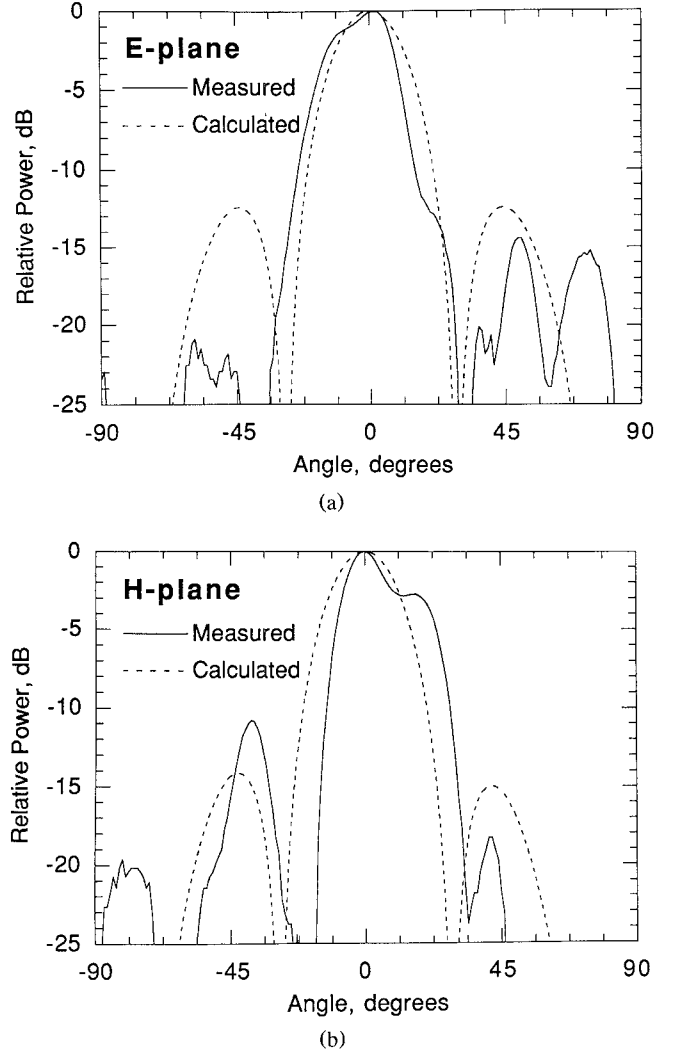


Fig. 9. (a)  $E$ -plane and (b)  $H$ -plane patterns at 9.6 GHz for the active array of Fig. 7. The theoretical results are calculated by combining the pattern of a single patch [20] with a  $4 \times 4$  array factor. The dielectric slab above the array ( $\epsilon_r = 4$ ) has a small effect on the patterns. Good qualitative agreement between the measured and calculated curves indicates that the elements are nearly in phase with similar amplitudes.

to an EIRP of 22 W. The overall dc to RF conversion efficiency was low, typical of Gunn diodes, around 1%.

#### B. $4 \times 4$ Array Using MESFET's

While the Gunn diode array has demonstrated the concept of power combining using the weakly coupled oscillators, the low efficiency would be a major disadvantage in many applications. Much higher efficiency, a larger tuning range, and better noise properties can be obtained using FET devices. Furthermore, the use of FET's also invites optical control of the array [29].

The experimental MESFET array is depicted in Fig. 10. The individual element design was previously discussed, and each uses a general-purpose Fujitsu device (FSX02). Half as many bias lines were used in this array design, with bias isolation between the elements provided by a six-turn coil. The gate resistor was found necessary to

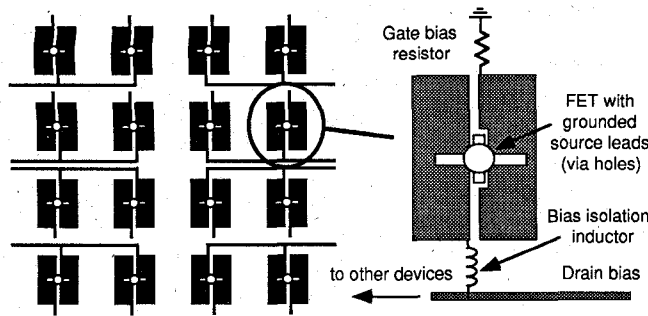


Fig. 10. Sketch of the array which uses Fujitsu fsx02 MESFET's, showing bias arrangement and individual element design. Elements measure 11 mm by 15 mm and the spacing of the elements is  $0.67\lambda_0$  between centers. The bias inductor reduces element interactions along the bias line.

suppress bias circuit oscillations. The array was fabricated on a 93 mil Duroid 5870 substrate ( $\epsilon_r = 2.33$ ).

As with the Gunn array, the power-on sequence was to tune each group of elements individually to set a common operating frequency, and then apply dc power to all elements at once. Varying the reflector element spacing is then usually sufficient to enforce mutual synchronization. With single-frequency operation verified at 8.27 GHz (within 3% of the 8 GHz design frequency) using a spectrum analyzer, the patterns of Fig. 11 were measured. These patterns closely correspond to the expected pattern when the elements are all in phase. Linear polarization is clearly indicated by the low cross-polarization levels. A maximum received power of 1.4 mW at a distance of 2.23 m was measured using a 19 dB pyramidal horn, yielding an EIRP of 10 W. A total radiated power of 184 mW was estimated from the pattern measurements, giving 11.5 mW per device at 26% efficiency. The corresponding directivity is 17.2 dB. The results of the MESFET array are seen to be similar to those of the Gunn array, but with a much higher dc-to-RF efficiency, which makes it a more attractive design. Better efficiency and somewhat higher output power per device could be obtained by using gate bias to each element.

The MESFET array exhibited a broader tuning range than the Gunn array, approximately 400 MHz with varying reflector position. Much quieter operation was also observed, which is characteristic of FET's. The spectrum of the MESFET array is shown in Fig. 12, along with the spectrum when the array is externally locked to an HP8350B sweeper (83592B plug-in). Phase noise of  $-78$  dB/Hz at 100 kHz for the free-running case was measured using a spectrum analyzer.

## VI. CONCLUSION

An architecture for quasi-optical power combining has been discussed which involves mutually synchronized arrays of single-device power sources. These elements integrate a device with a polar radiating element, such as a patch antenna. The oscillators are allowed to interact weakly in order to synchronize the frequency and phase relationships. A quasi-optical reflector element was found

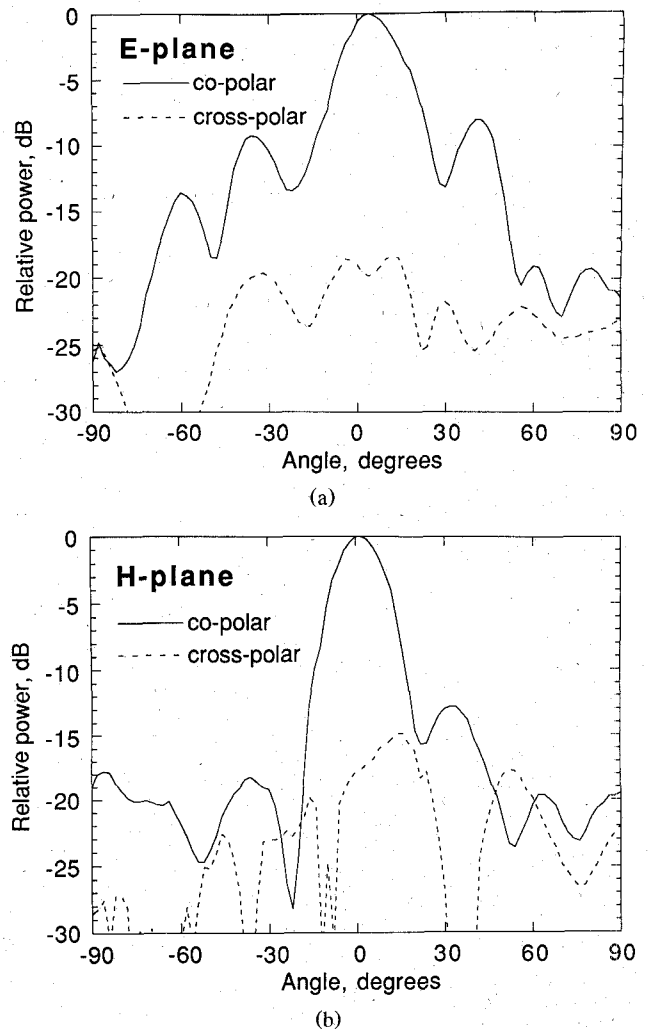


Fig. 11. (a) *E*-plane and (b) *H*-plane patterns for the  $4 \times 4$  MESFET array. The measurements were made at 8.27 GHz, using a flat, 2.5-cm-thick dielectric reflector with a dielectric constant of 4. The good patterns indicate in-phase operation.

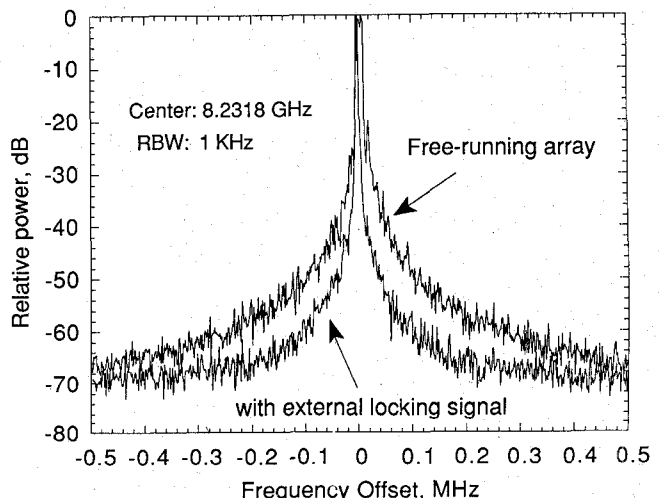


Fig. 12. Free-running and externally locked spectra of the MESFET array. The locking signal was injected through a pyramidal horn, which illuminated the array from a distance of 1 m.

to aid in establishing a desired phase relationship. By limiting the coupling to free-space interaction, the array design reduces to the design of a suitable single oscillator element. A simple theory based on Adler's equation has also been presented which establishes certain design guidelines for these types of arrays. Further work is necessary to incorporate the reflector element into the theory.

The proposed concepts have been verified using two 16-element X-band arrays, one utilizing Gunn diodes in patch antennas as the active element and the other using MESFET's. The Gunn diode array operated at 9.6 GHz with an EIRP of 22 W at 1% efficiency, while the MESFET array operated at 8.2 GHz with an EIRP of 10 W at 26% efficiency. Both of the arrays were constructed using hybrid assembly techniques. For large arrays, biasing will be an important issue. Proper operation of the array requires that the elements have nearly identical characteristics, which would allow them to be biased from a common source. Therefore, monolithic fabrication of millimeter-wave arrays is expected to be the best test of theory and design concepts presented here, and represents the next logical step in this area.

The main goal of this work is to develop a reliable, high-power solid-state source for the high millimeter-wave region, beyond 100 GHz. This will require hundreds or thousands of devices. Some existing theoretical work on quasi-optical power combiners indicates that there is a diminishing return as the number of devices increases [6]. Further experimentation is necessary to establish scaling laws for these arrays.

Future areas of research include beam steering and optical control of the arrays. Individual control of the elements becomes difficult because of limited real estate. Optical control provides a means of addressing each element and can be realized by using integrated detectors of direct illumination of MESFET's or HEMT's [29]. The optical signals may be used to provide RF modulation or phase control. Beam steering can be achieved by varying the coupling between elements. This is illustrated in Fig. 5, where the central beam changes considerably as the position of the reflector element is varied.

#### ACKNOWLEDGMENT

The authors are indebted to Prof. B. Z. Kaplan for helpful discussions regarding coupled oscillator theory, and to Prof. D. B. Rutledge at Caltech and Prof. K. D. Stephan at the University of Massachusetts for their advice and encouragement. Substrate material was donated by the Rogers Corporation and the MESFET's were donated by Fujitsu.

#### REFERENCES

- [1] J. W. Hansen, "U.S. TWT's from 1 to 100 GHz," *Microwave J.*, pp. 179-193, Sept. 1989.
- [2] Y. C. Shih and H. J. Kuno, "Solid-state sources from 1 to 100 GHz," *Microwave J.*, pp. 145-161, Sept. 1989.
- [3] K. Chang and C. Sun, "Millimeter-Wave Power-Combining Techniques," *IEEE Trans. Microwave Theory Tech.*, vol. MTT-31, pp. 91-107, Feb. 1983. Contains an extensive reference list on classical combining techniques.
- [4] K. Kurokawa, "The single-cavity multiple-device oscillator," *IEEE Trans. Microwave Theory Tech.*, vol. MTT-19, pp. 793-801, Oct. 1971.
- [5] J. W. McClymonds, Raytheon Research Division, private communication.
- [6] J. W. Mink, "Quasi-optical power combining of solid-state millimeter-wave sources," *IEEE Trans. Microwave Theory Tech.*, vol. MTT-34, pp. 273-279, Feb. 1986.
- [7] M. J. Wengler, A. Pance, B. Liu, and R. E. Miller, "Quasi-optical Josephson oscillator," *IEEE Trans. Magn.*, to be published.
- [8] Z. B. Popovic and D. B. Rutledge, "Diode-grid oscillators," in *Proc. 1988 IEEE AP-S Int. Symp.*, pp. 442-445.
- [9] Z. B. Popovic, R. M. Weikle, M. Kim, K. A. Potter, and D. B. Rutledge, "Bar-grid Oscillators," *IEEE Trans. Microwave Theory Tech.*, vol. 38, pp. 225-230, Mar. 1990.
- [10] H. J. Thomas, D. L. Fudge, and G. Morris, "Gunn source integrated with microstrip patch," *Microwave & RF*, pp. 87-89, Feb. 1985.
- [11] T. O. Perkins, "Active microstrip circular patch antenna," *Microwave J.*, pp. 110-117, 1987.
- [12] K. Chang, K. A. Hummer, and G. K. Gopalakrishnan, "Active radiating element using FET source integrated with microstrip patch antenna," *IEEE Trans. Microwave Theory Tech.*, vol. MTT-31, pp. 91-92, Sept. 1988.
- [13] N. Camilleri and B. Bayraktaroglu, "Monolithic mm-wave IMPATT oscillator and active antenna," *IEEE Trans. Microwave Theory Tech.*, vol. 36, pp. 1670-1676, Dec. 1988.
- [14] R. A. York, R. M. Martinez, and R. C. Compton, "Hybrid transistor and patch antenna element for array applications," *Electron. Lett.*, vol. 26, pp. 494-495, Mar. 1990.
- [15] M. R. Lakshminarayana and L. D. Partain, "Numerical simulation and measurement of Gunn device dynamic microwave characteristics," *IEEE Trans. Electron Devices*, vol. ED-27, pp. 546-552, March 1980.
- [16] K. Chang, K. A. Hummer, and J. L. Klein, "Experiments on injection-locking of active antenna elements for active phased and spatial power combiners," *IEEE Trans. Microwave Theory Tech.*, vol. 37, pp. 1078-1084, July 1989.
- [17] K. D. Stephan, "Inter-injection-locked oscillators for power combining and phased arrays," *IEEE Trans. Microwave Theory Tech.*, vol. MTT-34, pp. 1017-1025, Oct. 1986.
- [18] K. D. Stephan and W. A. Morgan, "Analysis of interinjection-locked oscillators for integrated phased arrays," *IEEE Trans. Antennas Propagat.*, vol. AP-35, pp. 771-781, July 1987.
- [19] R. Adler, "A study of locking phenomena in oscillators," *Proc. IRE*, vol. 34, pp. 351-357, June 1946; reprinted in *Proc. IEEE*, vol. 61, pp. 1380-1385, Oct. 1973.
- [20] K. Kurokawa, "Injection-locking of solid-state microwave oscillators," *Proc. IEEE*, vol. 61, pp. 1388-1409, Oct. 1973.
- [21] A. E. Siegman, *Lasers*. California: University Science Books, 1986. Chapter 19 offers an excellent discussion of injection locking, albeit in a different context than described here.
- [22] B. Z. Kaplan and K. Radparvar, "Canonic coupling of sinusoidal oscillators: New results," *Int. J. Systems Sci.*, vol. 16, no. 10, pp. 1257-1263, 1985.
- [23] B. Z. Kaplan and K. Radparvar, "Canonic coupling of oscillators in a chain," *J. Franklin Inst.*, vol. 325, no. 1, pp. 49-60, 1988.
- [24] K. D. Stephan and S. L. Young, "Mode stability of radiation-coupled interinjection-locked oscillators for integrated phased arrays," *IEEE Trans. Microwave Theory Tech.*, vol. 36, pp. 921-924, May 1988.
- [25] W. P. Shillue and K. D. Stephan, "A technique for the measurement of mutual impedance of monolithic solid-state quasi-optical oscillators," *Microwave and Opt. Tech. Lett.*, Dec. 1990.
- [26] R. A. York and R. C. Compton, "A 4×4 array using Gunn diodes," presented at IEEE Antennas Propagat. Symp. (Dallas), May 1990.
- [27] D. B. Rutledge *et al.*, "Quasi-optical power combining arrays," in *1990 IEEE MTT-S Int. Microwave Symp. Dig.* (Dallas), May 1990.
- [28] J. R. James, P. S. Hall, and C. Wood, *Microstrip Antenna Theory and Design*. London: Peter Peregrinus, 1981.
- [29] C. Rehwinkle *et al.*, "Optical control of MESFET and HEMT millimeter/microwave circuits," presented at 15th Int. Conf. Infrared and Millimeter Waves (Orlando), Dec. 1990.

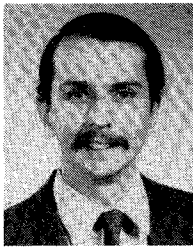
[30] M. Nakayama, M. Hieda, T. Tanaka, and K. Mizuno, "Multi-element quasi-optical oscillator arrays for terahertz region," in *Proc. Int. Symp. Space Terahertz Technol.* (Ann Arbor), Mar. 1990, pp. 377-379.



**Robert A. York** (S'86) received the B.S. degree in electrical engineering from the University of New Hampshire in 1987 and the M.S. degree from Cornell University in 1989 under a Schlumberger fellowship. Currently he is working towards the Ph.D. degree in microwave engineering at Cornell, studying millimeter-wave active arrays and power-combining techniques. His other research interests include microwave materials measurements and developing CAD methods for educational purposes.

Mr. York was the recipient of a 1990 IEEE MTT Graduate Fellowship Award and a corecipient of the Ban Dasher award for best paper at

the 1989 IEEE Frontiers in Education Conference. He is a student member of the Tau Beta Pi honor society.



**Richard C. Compton** (S'84-M'87) received the B.Sc. degree from the University of Sydney in 1983. During his Ph.D. studies, at the California Institute of Technology (1983-1987), he worked as a Fulbright scholar on several projects, including the design, fabrication, and measurement of millimeter and submillimeter-wave antennas and arrays. He codeveloped an interactive microwave CAD education package, *Puff*, which is used in microwave classes at universities worldwide.

His group at Cornell University is working on millimeter-wave integrated circuit design and on novel techniques for fabricating and measuring circuits at millimeter wavelengths. He has been a consultant for the Hughes Aircraft Company and TRW.

Dr. Compton is a National Science Foundation Presidential Young Investigator, and is an editor of the *IEEE Antennas and Propagation Magazine*.